J Current Pharma Sci. Res., 2024; 1(2):48-54.
https://jcpsr.com

Research Article

Atomistic Interplay of Remdesivir Bound SARS-CoV-2 Replicase and Thermodynamic Evaluation of Site-Directed Water Molecules: An Approach to Brownian Dynamics Simulation

Bedabrata Ray[1], Mohammed Rafi[2], Nipun Abhinav[3], Prasad Sunnapu[4,*]

[1]Department of Pharmaceutical Sciences, Amity Institute of Pharmaceutical Sciences, Amity University, Noida, Uttar Pradesh, INDIA.
[2]Department of Chemistry, AV College of Arts, Science and Commerce, Domalguda, Hyderabad, Telangana, INDIA.
[3]Department of Natural Products, Pharmaceutical Research Centre, Sanskriti University, Mathura, Uttar Pradesh, INDIA.
[4]Department of Pharmaceutical Chemistry, College of Pharmacy, Sri Ramakrishna Institute of Paramedical Sciences, Coimbatore, Tamil Nadu, INDIA.

ABSTRACT

Aim/Background: The replication-transcription complex (RTC) of SARS-CoV-2 plays a critical role in viral RNA synthesis and replication, primarily through the RNA-dependent RNA polymerase (RdRp). Remdesivir (RDV), a nucleotide analogue, inhibits RTC by disrupting nucleotide incorporation. However, understanding the detailed thermodynamic behaviour and conformational dynamics of the RdRp-RDV complex, including the role of catalytic site water molecules, remains crucial for guiding new antiviral development. **Materials and Methods:** We performed 100 ns of classical unbiased molecular dynamics (MD) simulation using the Desmond module of Schrödinger Suite (OPLS4 force field) on the SARS-CoV-2 RdRp-Remdesivir complex (PDB ID: 7bv2). Protein-ligand interaction analyses, metastable state clustering, and molecular mechanics/generalized Born surface area (MM/GBSA) calculations were conducted. The role of water molecules at the RdRp catalytic site was evaluated through solvent accessibility, water-bridge formation, and resolvation energy assessments. **Results:** The RdRp-RDV complex displayed minimal conformational fluctuations with stable ligand RMSD (~1.07 Å). Three metastable clusters were identified, with cluster 3 contributing 95% of the population and demonstrating the highest ligand binding stability. Key residues-Arg553, Arg555, Asp623, and Asp760-showed significant interaction sustainability via hydrogen bonds, ionic contacts, and water bridges. Water-mediated interactions notably contributed to binding stability, influencing ligand pose orientation. The average binding free energy (ΔG) was -28.99 kcal/mol, with key residues contributing strongly to system enthalpy. Water molecules at the active site provided additional stability, confirmed by free energy contributions ranging from 10.66 to 12.05 kcal/mol. **Conclusion:** This study elucidates the atomistic dynamics and thermodynamic profiling of the RdRp-RDV complex, highlighting the critical role of water molecules and specific amino acid residues in sustaining ligand binding. These insights offer strategic guidance for the rational design of next-generation RdRp inhibitors with enhanced pharmacodynamic profiles targeting SARS-CoV-2.

Keywords: RNA-Dependant RNA Polymerase, SARS-CoV-2, Solvation, Metastable State, Energy.

Correspondence:
Mr. Prasad Sunnapu
Department of Pharmaceutical Chemistry, College of Pharmacy, Sri Ramakrishna Institute of Paramedical Sciences, Coimbatore, Tamil Nadu, INDIA.
Email: prasadpharmachem@gmail.com

Received: 16-08-2024;
Revised: 12-12-2024;
Accepted: 03-07-2025.

INTRODUCTION

COVID-19 (Coronavirus Disease 2019), commenced as a devastating pandemic and humanitarian crisis, caused by Severe Acute Respiratory Syndrome Coronavirus 2 (SARS-CoV-2) which has by far propagated the infection among 640 million people, worldwide.[1,2] The prevalence of SARS-CoV-2 persists unceasingly in the form of variable lineages (Variants).[3] Besides, manifesting respiratory distress and disease-moderated symptoms, it causes impairment of consciousness, variable degrees of neuropathies, haemorrhagic and ischemic stroke, myalgia, convulsion, and encephalopathy.[4] In recent times, the World Health Organization has defined a new phenomenon of COVID-19 symptom reoccurrence after 3 months of disease recovery, as 'Long Covid'[5] or 'Post-Acute COVID-19 Syndrome' (PACS).[6] Morbidity and Mortality Weekly Report (2023-2024), the United States stated, the trial of vaccine efficacy on immunocompetent adults against

OPEN ACCESS

Manuscript TECHNOMEDIA

DOI: 10.5530/jcpsr.2024.1.2.8

Publishing Partner : Manuscript Technomedia. [www.mstechnomedia.com]

the newly introduced variant (Monovalent XBB.1.5). Henceforth, in mitigation of disease severity, antiviral drug design is the field of concerned research and the research of nation importance all around the globe. In management/as a therapeutic intervention of COVID-19, SARS-CoV-2 RNA-Dependant RNA Polymerase (RdRp) has been considered an enigmatic target for new antiviral drug discovery.[7] Furthermore, the active site of the viral (SARS-CoV-2) RdRp is highly conserved for most other species of virus[8] and thereby, targeting RdRp could be an approach of high excellence in the discovery of pan-viral inhibitors as nucleotide-binding analog. SARS-CoV-2 which employs positive-strand RNA as its genomic material, solely replicates by the functionalization of Replication-Transcription Complex (RTC) in catalytic mediation of RdRp.[9] The core of RTC is mainly comprised of the nonstructural protein 12 (catalytic subunit) of RdRp and its function is facilitated by other auxiliary components (nsp7, $nsp8_2$).[10,11] After the accomplishment of clinical success of Remdesivir (RDV), favipiravir, and molnupiravir, RTC receives pivotality as a pragmatic pharmacologically viable target for SARS-CoV-2 management.[12] Here we particularly and evidently investigate the atomistic interplay and dynamicity of Remdesivir Triphosphate (RTP/active metabolite of remdesivir) bound complex with RNA-dependant RNA polymerase of SARS-CoV-2 (PDB ID: 7bv2)[13] to gain the insights of the decisive role of solvation at the RTC binding site and to identify the key amino acid with the prior residency with its free-energy approximation. Faithful incorporation of natural Nucleotide Triphosphate (NTP) which is adenosine triphosphate, is stymied by the intervention of RTP at the site of nsp12 subunit of RdRp. RTP competitively binds with the Uracil-20(U20) nucleotide of nascent RNA by the formation of a covalent anchor and stalls the template elongation. Utilizing the computational simulation system, we tried to understand the conformational stability of the RdRp inhibitor-bound complex and segregated them into different population clusters to surface the role of water molecules in contact sustainability with backbone amino acid residues. We hereby utilized unbiased classic dynamics simulation (Brownian Dynamics) for the study of the behavioral investigation of the protein-inhibitor complex. Therefore, we anticipated that this study would facilitate the drug design and reveal new insights that could not be primarily understood by referring 2.50 Å RTP bound RdRp complex.

MATERIALS AND METHODS

Molecular Modeling

Classical unbiased Molecular Dynamics (MD) simulation,[14] molecular mechanics driven generalized born surface area (MM/GBSA),[15] and ligand binding site proximal resolvation energy analysis were performed using Maestro engine (version 2021-2, Schrödinger, LLC). The OPLS4 force field was palpably considered to conduct the different dimensions of modeling operandi. PyMol, a molecular graphics visualization system, was utilized to create numerous graphics to elucidate the atomistic interplay of the protein-ligand complex.[16]

MD Simulations

RNA-dependent RNA polymerase of SARS-CoV-2 complex with remdesivir (PDB ID: 7bv2) was utilized for assessment of MD simulation using the Desmond module of Schrödinger Suite. The respective protein-ligand complex was prepared with Protein Preparation Wizard. In the preprocess segment, bond-order correction, loop, and side-chain refinement were conducted using the prime algorithm. Henceforth, H-bond assignment and retrained minimization (0.60 Å RMSD) were implemented. Through the mediation of the Desmond simulation engine, a system builder was initiated to solvate the system with a TIP3P solvent model in a 10 Å boundary box construction. 4 Å region around the remdesivir binding site was excluded from the placement of salts and ions. Overall, 103413 atoms comprised the whole thermodynamic system with the addition of 0.15 M K^+ and Cl^- ions (purpose of system neutralization).[16] Finally, the built system was instigated to run in the NpT ensemble with a temperature of 300 K (isothermal/Nosé-Hoover method)[17] and a pressure of 1.01325 bar (isobaric/Martyna-Tobias-Klein method). Overall simulation course was set for 100 ns to evaluate the insights of the molecular interplay.

Protein-ligand interaction analysis

The overall trajectory of the 100 ns simulation course was analyzed using the simulation analysis tool of Desmond MD simulation engine (Schrödinger LLC). RMSD, RMSF, evolution of secondary structure elements, ligand proximal surface area analysis, and protein-ligand interaction residency were evaluated.[18] H-bond was considered with the distance calibration of 2.5 Å with the default angle standardization of ≥90° and ≥120° for the H-bond acceptor and donor, respectively. The automated default distance calibration for hydrophobic interaction, ionic bond, and water bridge (primary nature of interaction) were 3.6 Å-4.5 Å, 3.4 Å, and 2.8 Å respectively with a donor-acceptor angle profiling of ≥110° and ≥90°.

Interaction fingerprint and cluster analysis

The produced trajectory file from unbiased accelerated simulation was further proceeded for clustering using the interaction fingerprints algorithm (Schrödinger LLC). Fingerprint generation was conducted of the priorly generated 1000 frames of trajectory file and clustered them according to their structural conformational similarity. Following the methodology, the most dominant metastable conformation of the protein-ligand complex was identified and assured by distance matrix assessment.

Free Energy Analysis

The Molecular Mechanics-Generalized Born Surface area (MM-GBSA)[19] of the prime module of the Schrödinger Suite

was utilized for free energy (ΔG) calculation. Resolvation energy together with the energy contribution of the key amino acids with maximum contact residency time were calibrated with the functionalized solvation model of VSGB and OPLS4 force field.[20] Water molecules exhibiting stable contact sustainability were measured using the Hybrid Monte-Carlo algorithm.

RESULTS AND DISCUSSION

Atomistic interplay of remdesivir complexed with RNA bound RdRp

The rational introspection of our investigation deals with the development of understanding the influence of Brownian dynamics over covalently anchored remdesivir triphosphate at nsp12 enigmatic catalytic region of the RdRp RNA bound complex (Figure 1D). We performed unbiased classical molecular dynamics simulation which further castigated in illumination of new insights that cannot be inferred initially from cryo-electron microscopy (cryo-EM) snapshot of nsp12-nsp7-nsp8 bound RNA complex with the triphosphate chemical form of remdesivir. We here like to address the pertinence of ligand residency time at the catalytic site of nsp12 as well as the conformational stability and integrity of the protein-ligand complex to imply the ligand's (RNA-dependent RNA polymerase inhibitor) pharmacodynamic efficacy *in vivo*. Desmond engine-mediated MD simulation was conducted, and it culminated in the product of 100 ns simulation data. We considered no further extension of the simulation time course because the RMSD of protein backbone C-alpha was found to plateau (Supplementary Figure 1A). Covalently bound remdesivir was found extremely stable throughout the simulation trajectory. Initial 50 ns exhibited the protein C-alpha RMSD deviation ranging from 1.41 Å -2.26 Å and from there it escalates gradually up to 71 ns where the protein backbone RMSD became 2.34 Å. Thereafter, the RMSD graph of C-alpha remained plateaued which directly minor extent of conformational alterability of the RdRp protein backbone. In the last 30 ns, RMSD of C-alpha designated the value from 2.34 Å (lower limit) to 2.71 Å (upper limit). On the other side, RMSD of remdesivir triphosphate form appeared extremely stable and less deviating. On an average 1.07 Å ligand RMSD was measured in our study of MD simulation, and it that suggests a lesser degree of binding pose deviation from its reference frame (cryo-EM snapshot). RMSF measurement of RdRp protein backbone refers to remdesivir bound site is least deviating compared to other auxiliary components of protein (nsp7, nsp8, NiRAN, fingers, thumb, palm, and β-hairpin region) (Figure 1A). In RMSF representing a graph of RdRp backbone, the least deviating site was delineated with green-colored bands (Supplementary Figure 1). In this region, the contact between

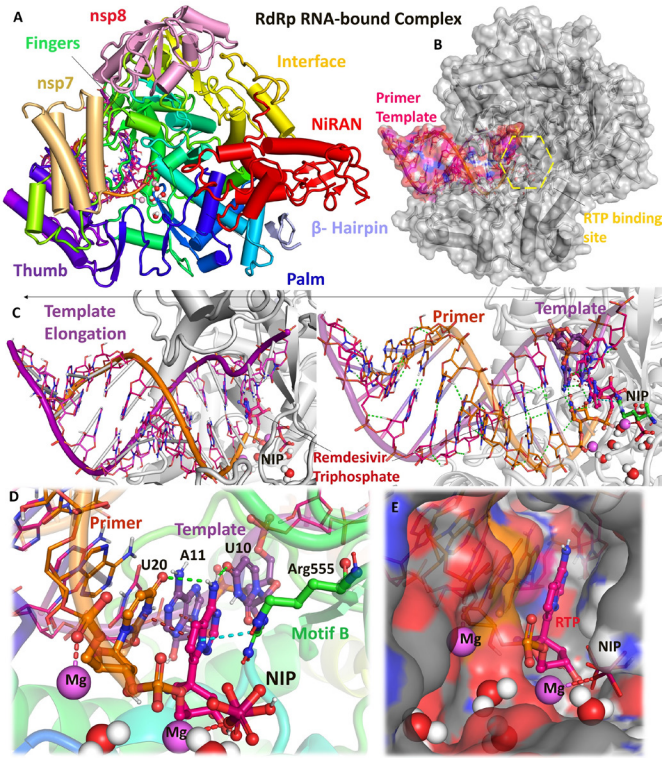

Figure 1: Overall architecture and binding orientation of remdesivir triphosphate (RTP) with RNA-bound conformation of RdRp with its core and auxiliary subunits. A and B, obtained from cryo-EM structure, is the absolute elucidation of delineating the discrete parts of RdRp with asymmetric color gamut. B. In this figure, RdRp is showcased in surface projection where the RTP binding region was highlighted with a dotted yellow colored hexagonal ring, and the primer-template attachment region was emphasized with transparent surface representation. C. Here the direction of template elongation was directed with an arrow. D. Prodrug remdesivir triphosphate binding pose was delineated with its key interactions with amino acids as well as nucleotides. RTP along with key amino acids/nucleotides were shown in the ball and stick model. Mg2+ is presented here in spheres at nsp12. Interactions between ligands and proteins were depicted in dotted lines. E. Delineation of scattered water molecules without any occurrence of water bridge formation..

remdesivir and RdRp was stabilized the most and further justified with the measured RMSF from 0.63 Å to 1.04 Å. Of note, as far as the drawn inference of reported cryo-EM structure, the delineated interactions were (1) covalent bond interaction between remdesivir triphosphate (the active form of RDV) with Uracil 20 (U20) of the primer, located nsp12 catalytic site, (2) π-cation interaction establishment between pyrrolo-triazine ring system and Arg555, (3) π- π stacking interaction formation between the pyrrolo-triazine and Uracil U20, adenine 11(A11) nucleotides of primer assemble as well as with uracil 10 (U10) of nascent template (Figure 1D). Intervention of site-directed water molecules was not observed but the presence of scattered water molecules was detected otherwise. Thereby, the immense pertinence of the study surfaces with its finding of the elucidated role of water molecules in binding orientation fixation at the core of RdRp. In our study, we highlight, the prominent contact sustainability with the nsp12 catalytic site residues, Arg555, Arg553, Thr680, Ala688, Asn691, Asp760, Asp623, and Lys545. Among these highlighted residues, we discovered Arg553, and Arg555 most stable in terms of contact residency time. Water bridge and ionic are the kinds of interactions that were found between remdesivir triphosphate and Arg553. Among these mode contacts, ionic interaction force sustained 79% and the water bridge persisted for 59% of the total simulation course. In the case of Arg555, H-bond, water bridge, and ionic linkage kind of interaction took place to manifest the contact consistency with the triphosphate form of remdesivir. The obtained result of MD simulation elucidated the persistence of 94.6%, 4%, and 71.5% for the H-bond, water-bridge, and ionic-bond interaction, respectively. In the case of Thr680, Ala688, Asn691, Asp760, Asp623, and Lys545, water-bridge has emerged as the major contributor in contact residency with RTP (Supplementary Figure 1D). Therefore, these findings directly infer the importance of contact consistency with Arg553, Thr680, Ala688, Asn691, Asp760, Asp623, and Lys545 that was not propagated from the preliminary reference frame (cryo-EM conformation). This facilitates the structure-based drug design and discovery in case of prior targeting to improve drug susceptibility, selectivity, and pharmacodynamic profiling.

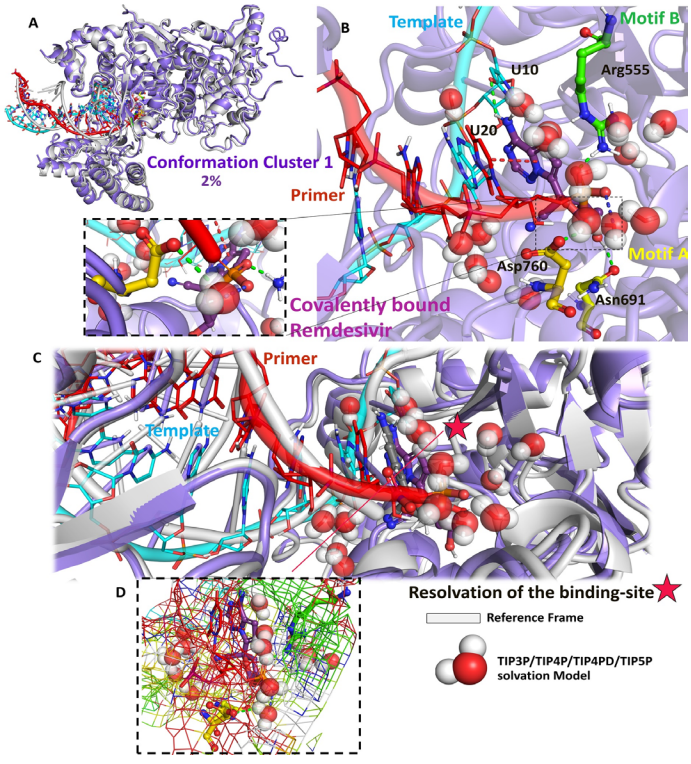

Figure 2: Metastable state (cluster 1) of RdRp remdesivir complex. A. The delineation of the first metastable state and its conformational topology. RdRp template bound complex is depicted in the cartoon where the RdRp is represented in marine blue and template-primer conjugation is shown in cyan and bright red respectively. B. Elucidation of interaction establishment with the nucleotides of primer as well as template and backbone amino acid at motif A/ motif B. C. Representation of water molecule density at the binding site of RTP. Water molecules are hereby represented in a sphere. D. Depiction of proximity region of RTP located site and it was represented in mesh projection..

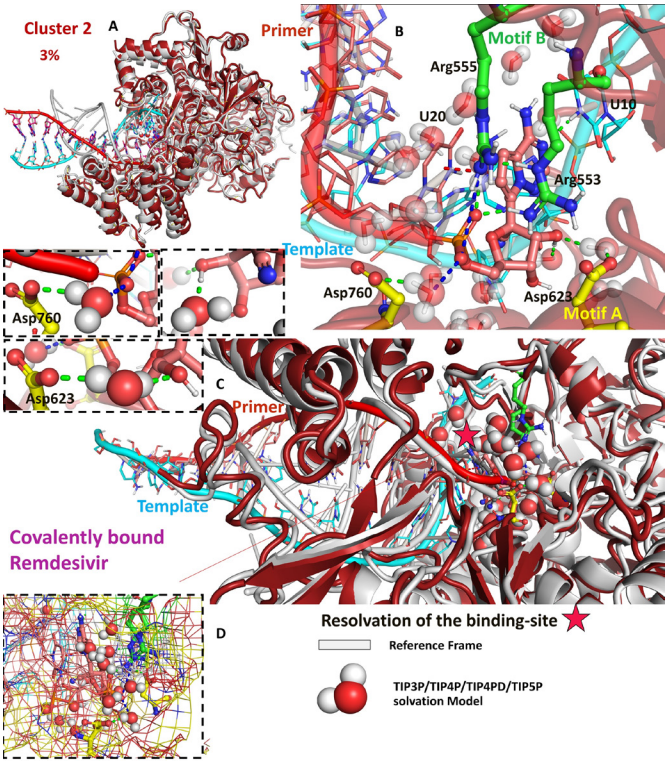

Figure 3: Structural representation of cluster 2 (a prior metastable state) and intervention of water molecules in ligand's binding orientation sustainability. A. Representation of RdRp conformational specificity with covalently bound remdesivir. Here protein is represented in brick red. B. Interaction residency with backbone amino acids as well as with the nucleotides of primer-template conjugation. Key amino acid residues are projected in the ball & stick with the variable color gamut according to their motif-specific location site. C. Representation of the density of water molecules at RTP binding-site location. Here, water molecules participated in salt-bridge formation and otherwise interaction with the ligand are separately highlighted. D. Elucidation of the vicinity location of RTP binding in the mesh..

Metastable state distribution and conformational dynamics

Overall simulation framework was utilized to isolate the significant dynamic behaviour of the protein-ligand complex and thereby, we resenect the conformation alterability and shiftment from its initial shape and orientation. Although previously it was discussed that obtained RMSD and RMSF imply a minute protein conformational deviation and limited extent of local site perturbation (RTP binding-site). Despite the protein conformational stability, some degree of adjustment and dynamicity was observed in remdesivir binding pose orientation. Binding mode variability of remdesivir, delineated the inclusion of numerous amino acids from different motif sites of the RdRp-template bound structure. Now in the process of establishing the priority and relevance of protein-ligand associated conformational dynamicity, we utilized interaction fingerprinting, shape similarity identification, and the canvas algorithm for clustering of dominant metastable states. Henceforth, we identified three discrete conformation state/ metastable states which were heightened in our study as cluster 1 (marine blue), cluster 2 (brick red), and cluster 3 (olive green). Population contribution of these three states was unequally distributed. Cluster 1 confirmed the least (1%) contributor of total protein-ligand conformation population, attained from the simulation timeline (Figure 2). On the other hand, cluster 2 contributed 3% of the total population on the grounds of shape and interaction residency (Figure 3). Followed by clusters 1 and 2, cluster 3 has emerged as the most dominant contributor. In the case of cluster 3, it comprises 95% of the total RdRp-RTP complex population (Figure 4). The amino acids that were found in the state interacting with RTP, demand prior attention in Structure-Based Drug Designing (SBDD). In cluster 3, the binding site of RTP was also observed most populated and crowded with the presence of water molecules and maximum water bridge formation with the discussed backbone amino acids along with its residency were found in our keen investigation (Figures 4A-D). In our study of thermodynamic parameters, the exhibition of free binding energy (ΔG) for RTP was found most electrostatically viable and its Gibbs free energy ranged from 30.96 -27.02 kcal/mol. It in practice directs the thermodynamic favourability of cluster 3 as a prevalent metastable circumstance.

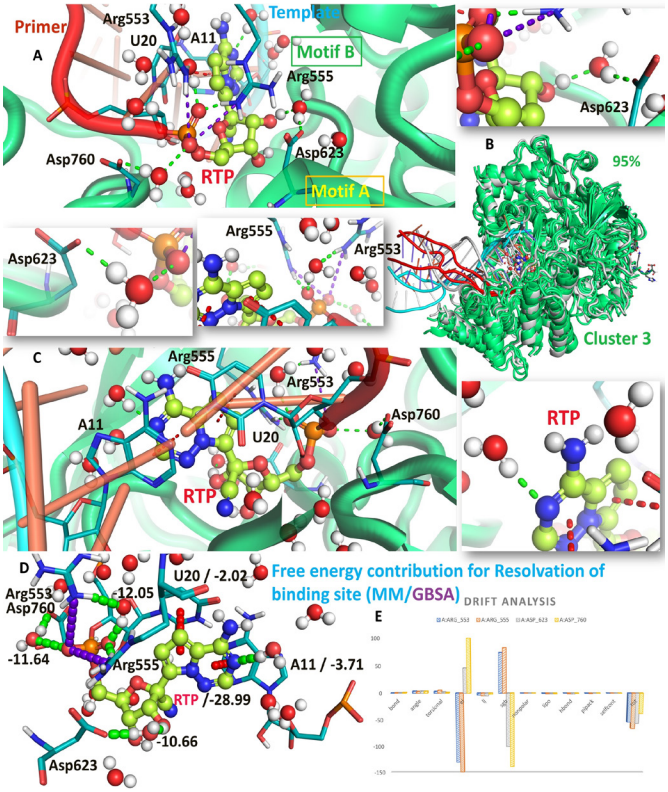

Figure 4: Structural architecture of the most populated metastable state and its thermodynamic profiling. A. and C. Overall demonstration of pertinent interactions of RTP at RdRp catalytic site. B. Structural orientation of cluster 3 superimposed with reference frame (delineated in white color projection). D. Free-binding energy contributed by different backbone amino acids, nucleotides, and water molecules was displayed. E. Deciphering drift analysis to showcase the definite energy contribution of key amino acid residues..

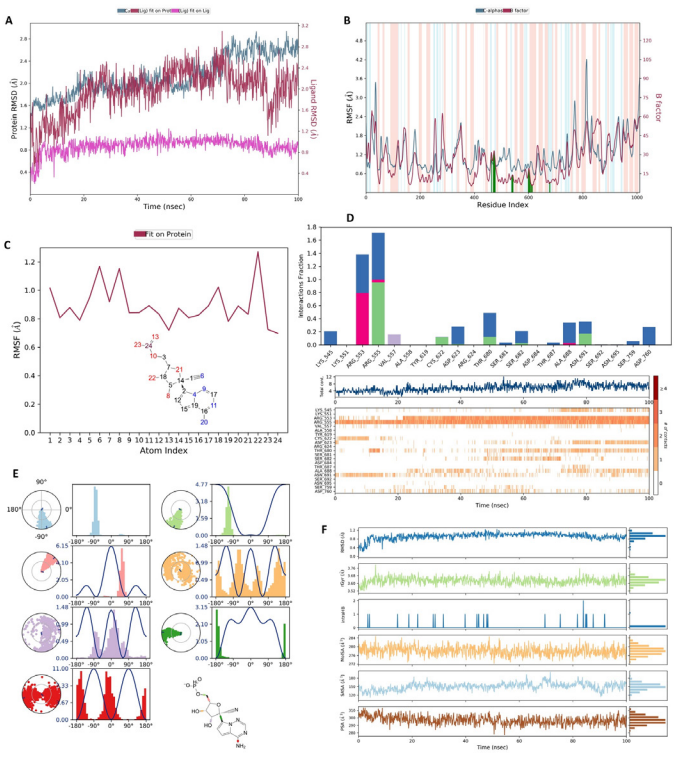

Figure S1: The wholistic representation of the outcome of the performed unbiased MD simulation. A. The depiction of the RMSD of SARS-CoV-2 replicase (RdRp). B. The portrayal of the RMSF of RdRp along with the distinction of the secondary structure element. Here, the green bands specifically highlight the contact points between RdRp and covalently bound remdesivir triphosphate (RTP). C. Representation of remdesivir atomic fluctuation. D. Deliberate direction of contact residency of RTP with the respective amino acids at the catalytic core of RdRp. E. Depiction of torsion angle profile of RTP. F. Simulated result of ligand properties, like RMSD, radius of gyration (rGyr), intraHB (intra-atomic hydrogen bond formation), MoISA, SASA, and PSA..

Interaction sustainability and contact discrepancy among the metastable states

In our study, we particularly identified three discrete states out of the dynamistic interplay of the RdRp-RTP complex. In this investigation, we primarily aimed to direct the backbone residues that contributed pivotally to the binding mode residence of RTP at the catalytic core of RdRp. We thereby were driven to seek the key amino acids that are important from the point of interaction sustainability and ligand binding mode consistency but were not surface from the preliminary inspection of the available cryo-EM structure of RdRp template bound complex with RTP. It indeed causes derogation of the drug design approach targeting RdRp to stall the nascent template production. In our effort to impart clarity and facilitate site-directed drug discovery, we analyzed the prior contact consistency among all three considerable clusters. In cluster 1, apart from irreversibly bound with U20 of the primer, the found interactions between remdesivir triphosphate and the catalytic site of RdRp were (1) H-bond interaction between the attached amino group (-NH_2) of pyrrolo-triazine and U10 of the nascent formed template, (2) H-bond interaction between the hydroxy group of oxolan and Asn691 at motif A, (3) water molecule mediated contact (water-bridge) between methoxy hydroxy phosphoryl and Asp760 at motif A, (4) H-bond interaction between the hydroxy group pf oxolan and Arg555 at motif B, and (5) H-bond interaction between a proximal water molecule and oxolan ring system (Figure 2B). Most of the amino-acid-specific interactions, displayed in cluster 1, remained in cluster 2. In cluster 2, the most dominant interactions were found established (1) H-bond interaction between methoxy hydroxy phosphoryl group with Arg555 and Arg553 at motif B region, (2) water bridge formation between methoxy hydroxy phosphoryl group and Asp760, (3) another occurrence water molecule mediated interaction between the hydroxy group of oxolan ring and Asp623 at motif A, and (4) U10 of nascent template was also found in contact with pyrrolo-triazine ring via H-bond (Figure 3B). The result of interaction assessment in cluster 1 and cluster 2, was found sustained in cluster 3 with some variability. The state of cluster 3 firmly signifies the pivotal role of water at the catalytic site of RdRp to facilitate RTP binding pose consistency. Unlike cluster 2, Arg553 interacted with methoxy hydroxy phosphoryl group via ionic (cation-anion interaction). On the other hand, interaction with Arg555 remained static. Similar kinds of water bridge-mediated interactions were found with Asp760 and Asp623 (Figures 4A and 4D). We found remdesivir with a higher value of Polar-Surface Area (PSA), Solvent Accessible Surface Area (SASA), and a significant value of the molecular ionizable surface area of 302.07 $Å^2$, 154.68 $Å^2$, and 280.88 $Å^2$ on an average respectively, we examined RTP proximal site of binding with the higher crowd of water molecules (Supplementary Figure 1F). Pyrrolo-triazine ring and hydroxy group of oxolan ring were found to have interacted with site-located water molecules that thereby employ a higher degree of ligand stability inbound orientation. The whole projection overall affirms the significant role of water at the catalytic binding core and higher exposure of water molecules therefore imposes further stability and states undoubtedly contributing to ligand binding.

Solvation energy approximation and free-energy contribution

Solvation energy is primarily an important and considerable parameter to facilitate the process of ligand optimization. Escalation of entropy and compensation of the enthalpy loss is deeply related to the liberation of water from the site, attained by an inhibitor or an instigator (agonist/partial agonist). Interaction mediation through site-located water molecules or dissociation of water molecules via the hydrophobes (hydrophobic warhead of a molecule) may have a direct impact on the biological function of a protein through activation aggregation. Therefore, alchemical water molecules present at the catalytic core of RdRp establishing contacts/working like a contact bridge projection, need to be evaluated on the ground of thermodynamic parameter. Besides, the binding potency of a molecule is a considerable feature for drug optimization to make it more thermodynamically viable. Here in our study, we investigated the binding free energy of covalently anchored remdesivir using MM/GBSA algorithm and it represented the free energy association of 28.99 kcal/mol (an average value throughout the simulation course) where Surface Generalized Born (sgb) and electrostatic energy (el) were the major contributor with the value of -34.03 kcal/mol and -10.45 kcal/mol, respectively (Figure 4E). Such an outcome implies its thermodynamic credential and can be opted as a reference point to assist further potent RdRp inhibitor development. Free-energy associations with major interacting amino acids (Arg553, Arg555, Asp623, and Asp 760) were examined explicitly. Arg553, Arg555, Asp623, and Asp 760 showed an energy contribution of -54.02 kcal/mol, -65.91 kcal/mol, -56.23 kcal/mol, and 37.58 kcal/mol chronologically. This demonstration of energy distribution, el is the major contributor to net-binding free energy association. Now the alchemical water molecules mediating the contacts of RTP with highlighted amino acids were also evaluated energetically. Free binding energy associated with those particular water molecules (participating in water bridge formation) ranged from 10.66 kcal/mol - 12.05 kcal/mol. This portrays the overall picture of the thermodynamic stature of the RTP-RdRp complex system in the solvation model and the pertinent contribution of water molecules to achieve the binding mode sustainability of RTP at the site of the RdRp catalytic core.

CONCLUSION

Lack of site specificity, efficacy, and off-target effect are those humongous hurdles we need to overcome in the field of clinical management. Lack of pharmacodynamic potential and compromised pharmacokinetic parameters are accompanied by the recurring clinical trial failure of numerous drug candidates.

Contact residency and, the dissociation/association profile of a molecule are important parameters to explore with utter sincerity. To cater to that sense of responsibility, in our study we investigated the atomistic interplay and the contact residency of the RdRp-RTP complex. From this study, we understood and highlighted some key MM/QM behaviour of the protein-ligand complex via the treatment of Brownian dynamics. We therefore direct the pivotality of contact residency with Arg555, Arg553, Asp623, and Asp760 that could not be inferred from the preliminary cryo-EM structural assessment of template bound RdRp-RTP complex. We deciphered the diligent role of water molecules in the pose orientation of RTP at the site of the catalytic core. Along with the understanding development of protein-ligand complex dynamicity, we evaluated the free-binding energy (ΔG) of backbone amino acids, and water bridge forming water molecules to exemplify the enthalpy stature of the thermodynamic system. Overall, our research finding will be hopefully castigated into the development of pharmacodynamically potent RdRp inhibitors with the improved residency profile pragmatically.

CONFLICT OF INTEREST

The authors declare that there is no conflict of interest.

REFERENCES

1. Wang, Z. *et al.* Naturally enhanced neutralizing breadth against SARS-CoV-2 one year after infection. *Nature*, 2021; 595: 426-31.
2. Holmes, E. C. COVID-19-lessons for zoonotic disease. Science, 1979; 375: 1114-5 (2022).
3. Kumar, P., Sobhanan, J., Takano, Y. and Biju, V. Molecular recognition in the infection, replication, and transmission of COVID-19-causing SARS-CoV-2: an emerging interface of infectious disease, biological chemistry, and nanoscience. *NPG Asia Mater*, 2021; 13: 14.
4. Desai, A. D., Lavelle, M., Boursiquot, B. C. and Wan, E. Y. Long-term complications of COVID-19. *American Journal of Physiology-Cell Physiology*, 2022; 322: C1-C11.
5. Ruf, W. Immune damage in Long Covid. *Science*,1979;383: 262-3 (2024).
6. Ramírez-Vélez, R. *et al.* Reduced muscle strength in patients with long-COVID-19 syndrome is mediated by limb muscle mass. *J Appl Physiol*, 2023; 134: 50-8.
7. Hillen, H. S. *et al.* Structure of replicating SARS-CoV-2 polymerase. *Nature*, 2020; 584: 154-6.
8. Charon, J., Buchmann, J. P., Sadiq, S. and Holmes, E. C. RdRp-scan: A bioinformatic resource to identify and annotate divergent RNA viruses in metagenomic sequence data. *Virus Evol*, 2022; 8.
9. Yan, L. *et al.* Architecture of a SARS-CoV-2 mini replication and transcription complex. *Nat Commun*, 2020; 11: 5874.
10. Stevens, L. J. *et al.* Mutations in the SARS-CoV-2 RNA-dependent RNA polymerase confer resistance to remdesivir by distinct mechanisms. *Sci Transl Med*, 2022; 14.
11. Gao, Y. *et al.* Structure of the RNA-dependent RNA polymerase from COVID-19 virus. *Science*, 1979; 368: 779-82 (2020).
12. Williamson, B. N. *et al.* Clinical benefit of remdesivir in rhesus macaques infected with SARS-CoV-2. *Nature*, 2020; 585: 273-6.
13. Yin, W. *et al.* Structural basis for inhibition of the RNA-dependent RNA polymerase from SARS-CoV-2 by remdesivir. Science, 1979; 368: 1499-1504 (2020).
14. Pantsar, T. *et al.* Decisive role of water and protein dynamics in residence time of p38α MAP kinase inhibitors. *Nat Commun*, 2022; 13: 569.
15. Wang, E. *et al.* VAD-MM/GBSA: A Variable Atomic Dielectric MM/GBSA Model for Improved Accuracy in Protein-Ligand Binding Free Energy Calculations. *J Chem Inf Model*, 2021; 61: 2844-56.
16. Ray, B. and Roy, K. K. Deciphering insights into the binding mechanism and plasticity of Telacebec with *M. tuberculosis* cytochrome *bcc-aa3* supercomplex through an unbiased molecular dynamics simulation, free-energy analysis, and DFT study. *J Biomol Struct Dyn*, 2023; 1-14.doi:10.1080/07391102.2023.2294833.
17. Leini, R. and Pantsar, T. *In Silico* Evaluation of the Thr58-Associated Conserved Water with KRAS Switch-II Pocket Binders. *J Chem Inf Model*, 2023; 63: 1490-505.
18. Roy, K. K., Jyothi, D., Paul, U. and Sukla, S. Identification and validation of novel non-nucleoside class of molecules inhibiting the dengue virus replication. *J Biomol Struct Dyn*, 2023; 41: 13993-4002.
19. Gaillard, T. and Simonson, T. Full Protein Sequence Redesign with an MMGBSA Energy Function. *J Chem Theory Comput*, 2017; 13: 4932-43.
20. Lu, C. *et al.* OPLS4: Improving Force Field Accuracy on Challenging Regimes of Chemical Space. *J Chem Theory Comput*, 2021; 17: 4291-300.